

## Second-Harmonic Generation in Odd-Period, Strained, $(\text{Si})_n(\text{Ge})_n/\text{Si}$ Superlattices and at Si/Ge Interfaces

Ed Ghahramani,<sup>(1)</sup> D. J. Moss,<sup>(2)</sup> and J. E. Sipe<sup>(1)</sup>

<sup>(1)</sup>*Department of Physics and Ontario Laser and Lightwave Research Centre, University of Toronto, Toronto, Ontario, Canada M5S 1A7*

<sup>(2)</sup>*National Research Council of Canada, Ottawa, Ontario, Canada K1A 0R6*

(Received 21 March 1990)

We report the first full band-structure calculation of frequency-dependent second-harmonic generation in odd-period  $(\text{Si})_n(\text{Ge})_n$  superlattices. We use these results in conjunction with a simple model to estimate second-harmonic generation at Si/Ge interfaces.

PACS numbers: 78.65.Gb, 73.20.Dx, 73.40.Lq

Optical second-harmonic generation (SHG) is forbidden in a medium with inversion symmetry, such as bulk Si or Ge, within the dipole approximation. But at a surface, or at an interface between two such media, the inversion symmetry is broken and SHG is allowed. Thus, SHG has been studied as a surface-specific optical probe.<sup>1,2</sup> Yet, except for some model calculations of SHG from metallic surfaces<sup>3,4</sup> which are far from realistic, no microscopic calculations have been attempted for surfaces or interfacial systems.<sup>5</sup> In this Letter we propose a new approach to the study of interfacial SHG in semiconductor superlattices where the density of interfaces is high.

Here we report the first full band-structure calculation of dipole-allowed SHG from odd-period  $(\text{Si})_n/(\text{Ge})_n$  superlattices. As expected, as  $n$  increases the calculated SHG decreases. Thus, the  $(\text{Si})_n/(\text{Ge})_n$  structures provide a way of studying the transition of allowed SHG from its nature in  $\text{Si}_1\text{Ge}_1$ , where we find it is comparable to bulk materials such as GaAs which have no inversion symmetry, to its nature in  $\text{Si}_5\text{Ge}_5$ , where it approaches the sum of contributions from a series of separated interfacial regions. Interpreting the results with a simple model, we can deduce a prediction for the allowed SHG from a single Si/Ge interface.

The SHG is also of interest from the point of view of

superlattice physics. Calculations of the dielectric tensor  $\epsilon(\omega)$  of the  $(\text{Si})_n/(\text{Ge})_n$  superlattices show that, except for very weak absorption due to the zone-folded states, the linear optical response can be thought of as an average of the linear responses of bulk Si and Ge.<sup>6</sup> The SHG response in the odd-period  $(\text{Si})_n/(\text{Ge})_n$  superlattices, on the other hand, has no counterpart in bulk Si and Ge. As such, it is truly a "pure superlattice" property.

Like bulk Si and Ge, the  $(\text{Si})_m/(\text{Ge})_n$  superlattices possess inversion symmetry for  $n$  and  $m$  even. Thus, in the limit of many interfaces within a wavelength, SHG is forbidden. We therefore concentrate here on the odd-period superlattices. In a recent publication<sup>6</sup> we carried out a full band-structure calculation of the linear optical properties of these superlattices, using a semi-*ab initio* linear combination of Gaussian orbitals technique in conjunction with the *X $\alpha$*  method for constructing the potentials of the constituent *bulk* materials. In our approach we do not do any fitting to the superlattice properties and our energy band-structure calculations<sup>6</sup> are in good agreement with experimental measurements.<sup>7,8</sup> In this paper we use the same energy band-structure and momentum matrix elements.

To calculate the second-order phase response, we use perturbation theory with the minimal-coupling interaction Hamiltonian, and we find

$$\chi^{(2)}(-2\omega; \omega, \omega) = \frac{i}{2} \left| \frac{e}{m\omega} \right|^3 \sum_{i,j,l} \int_{\text{BZ}} \frac{d\mathbf{k}}{4\pi^3} \frac{p_{ij}p_{jl}p_{li}}{2E - E_{ji}} \left[ \frac{f_{il}}{E - E_{li}} + \frac{f_{jl}}{E - E_{jl}} \right], \quad (1)$$

within the independent-particle approximation,<sup>9</sup> where  $E = \hbar\omega$ ,  $E_{ji} = E_j - E_i$ ,  $f_{ij} = f_i - f_j$ , etc., and  $f_i$  is the Fermi occupation factor of the single-particle state  $i$ . The  $p_{ij}$  are momentum matrix elements; indices  $i, j, l$  run over all single-particle states, the only restrictions arising from the Fermi factors. Equation (1) seems to indicate that  $\chi^{(2)}$  diverges in the limit of  $\omega \rightarrow 0$ . Aspnes<sup>10</sup> has shown that once Eq. (1) is decomposed into divergent terms and a finite term, the former vanish identically for materials with cubic symmetry. More generally, we

have derived new sum rules and can show that all divergent terms vanish independent of the crystal symmetry for filled valence bands. Once the divergent terms are removed, we expand the finite term using the Fermi factors and algebraically simplify the expression. We then explicitly write the contributions of the virtual-electron ( $i$  is the valence,  $j$  and  $l$  are the conduction states) and virtual-hole ( $i$  and  $l$  are the valence,  $j$  is the conduction states) processes<sup>10</sup> and separate the real and imaginary

parts of the expression in the usual manner by putting  $E = \hbar\omega + i\eta$  and taking the limit  $\eta \rightarrow 0^+$ . The contribution of the virtual-electron term to the imaginary part of the response is found to be

$$\chi''_{ve}{}^{(2)}(2\omega; -\omega, -\omega) = -\frac{\pi}{2} \left| \frac{e\hbar}{m} \right|^3 \sum_{i,j,l} \int_{\text{BZ}} \frac{d\mathbf{k}}{4\pi^3} \left[ \frac{p_{jl}^{cc} p_{ij}^{cc} p_{li}^{cc} \delta(E_{li} - \hbar\omega)}{E_{li}^3 (E_{li} + E_{ji})} - \frac{p_{ij}^{cc} p_{jl}^{cc} p_{li}^{cc} \delta(E_{li} - \hbar\omega)}{E_{li}^3 (2E_{li} - E_{ji})} + \frac{16 p_{ij}^{cc} p_{jl}^{cc} p_{li}^{cc} \delta(E_{ji} - 2\hbar\omega)}{E_{ji}^3 (2E_{li} - E_{ji})} \right], \quad (2)$$

where, e.g.,  $p_{ij}^{cc}$  is a momentum matrix elements between a valence state  $i$  and conduction state  $j$ . The virtual-hole term can be obtained from Eq. (2) by the following exchanges:  $E_{li} \rightarrow E_{jl}$ ,  $p_{li}^{cc} \rightarrow p_{jl}^{cc}$ ,  $p_{jl}^{cc} \rightarrow p_{li}^{cc}$ , and by having the index  $l$  run over valence states. There is also an extra overall minus sign in the virtual-hole term, arising from the anticommutation relations.<sup>9</sup> As seen from Eq. (2), resonances can occur when either  $\omega$  or  $2\omega$  is the frequency difference between two single-particle states.

To evaluate Eq. (2), we utilize the symmetry group of these superlattices and reduce the integral over the Brillouin zone (BZ) to an integral over its irreducible segment. This integral is then performed using a sampling method. Once we have evaluated  $\chi''^{(2)}$ , we use a Kramers-Kronig relation to obtain the real part of  $\chi^{(2)}$  and then calculate its magnitude; we include both the virtual-electron and virtual-hole contributions to the response. The magnitudes of the two independent components of  $\chi^{(2)}$  ( $\chi_{123}^{(2)}$  and  $\chi_{321}^{(2)}$ ) as a function of frequency are presented in Fig. 1. In Table I we present their magnitudes at zero frequency.

Examining the  $\omega$ - and  $2\omega$ -term contributions [Eq. (2)] to these results, we find that the first peak (around 1.3 eV) is due to the  $2\omega$  resonance with the bulklike  $E_1$  optical peak. The second peak (around 2.7 eV) is due to the sum of the  $\omega$  resonance with the bulklike  $E_1$  optical peak and the  $2\omega$  resonance with the bulklike  $E_2$  optical peak.<sup>6</sup> Therefore, most of the structure in  $\chi^{(2)}$  arises from transitions to bulklike, rather than zone-folded, conduction states. This is not surprising since the matrix elements between valence-band and zone-folded conduction-band states are generally 5–20 times smaller than those between valence-band and bulklike conduction-band states.<sup>6</sup> Yet, unlike the results for  $\epsilon(\omega)$  where the response due to the bulklike states can be understood for the most part as an average of the responses due to such states in the constituent bulk materials,<sup>6</sup> here the modification of the bulklike states due to the interfacial is crucial, since bulk Si and Ge do not allow dipole SHG.

To try to model how the SHG arises from the interfaces in a simple way, which will also help us to understand the decrease in  $\chi^{(2)}$  as  $n$  increases, we use a bond orbital model. In this model we consider SHG to arise locally at the Si–Ge bonds where the inversion symmetry is clearly broken. Assuming the electrons respond only by moving along the bond direction  $\hat{\mathbf{b}}$  (pointing from Si to Ge), we take the dipole moment induced at

$2\omega$  to be given by

$$\mu(2\omega) = \beta(\omega) \hat{\mathbf{b}} [\hat{\mathbf{b}} \cdot \mathbf{E}(\omega)]^2, \quad (3)$$

where  $\beta(\omega)$  is a nonlinear response coefficient. For any structure, we can estimate the SHG by summing up contributions [Eq. (3)] from all the Si–Ge bonds. In particular, for an  $(\text{Si})_n/(\text{Ge})_n$  superlattice with a coordinate system chosen so that a Si atom is at the origin and a Ge atom is at  $(\frac{1}{4}a_\perp, \frac{1}{4}a_\perp, a_{SG})$ , where  $a_\perp$  is the lattice constant in the plane perpendicular to the superlattice axis and  $a_{SG}$  is the spacing between a Si and Ge layer, we find

$$\chi_{ijk}^{(2)}(-2\omega; \omega, \omega) = \begin{cases} \frac{16\beta(\omega)}{na_\perp^3(2+\sigma^2)^{3/2}}, & i \neq j \neq k, \\ 0, & \text{otherwise,} \end{cases} \quad (4)$$

where  $\sigma = 4a_{SG}/a_\perp$ . There is much cancellation between terms of the form (3) in Eq. (4); indeed, for an *even*-period superlattice we find  $\chi^{(2)} = 0$  as expected. Note that Eq. (4) predicts that the magnitude of responses for  $n=3$  and 5 should be one-third and one-fifth, respectively, of the response for  $n=1$ , roughly in agreement with the results presented in Fig. 1 and Table I; this results simply because the density of interfaces for  $n=3$  and 5 are, respectively,  $\frac{1}{3}$  and  $\frac{1}{5}$  of the density of interfaces for  $n=1$ . Equation (4) also predicts  $\chi_{123}^{(2)} = \chi_{321}^{(2)}$ , which we can see from Fig. 1 is satisfied to within about 50%; this indicates the degree to which the model is valid.

We use the same model of Eq. (3) to estimate the interface second-order susceptibility  $\chi^{(I)}$  (in units of bulk second-order susceptibility per unit area) of a *single* Si/Ge interface. We find

$$\chi_{ijk}^{(I)}(-2\omega; \omega, \omega) = \begin{cases} \frac{4\beta(\omega)\sigma}{a_\perp^2}, & i, j, k \text{ not all equal,} \\ \frac{4\beta(\omega)\sigma^2}{a_\perp^2}, & i = j = k (\equiv z), \\ 0, & \text{otherwise,} \end{cases} \quad (5)$$

where  $\hat{\mathbf{z}}$  points from the Si to the Ge atom. Obtaining  $\beta(\omega)$  by setting the band-structure calculations for  $\frac{2}{3}\chi_{123}^{(2)} + \frac{1}{3}\chi_{321}^{(2)}$  equal to the right-hand side of Eq. (4), we then find  $\chi^{(I)}$  using Eq. (5). The results of this calculation for the term in the first line of Eq. (5) are presented

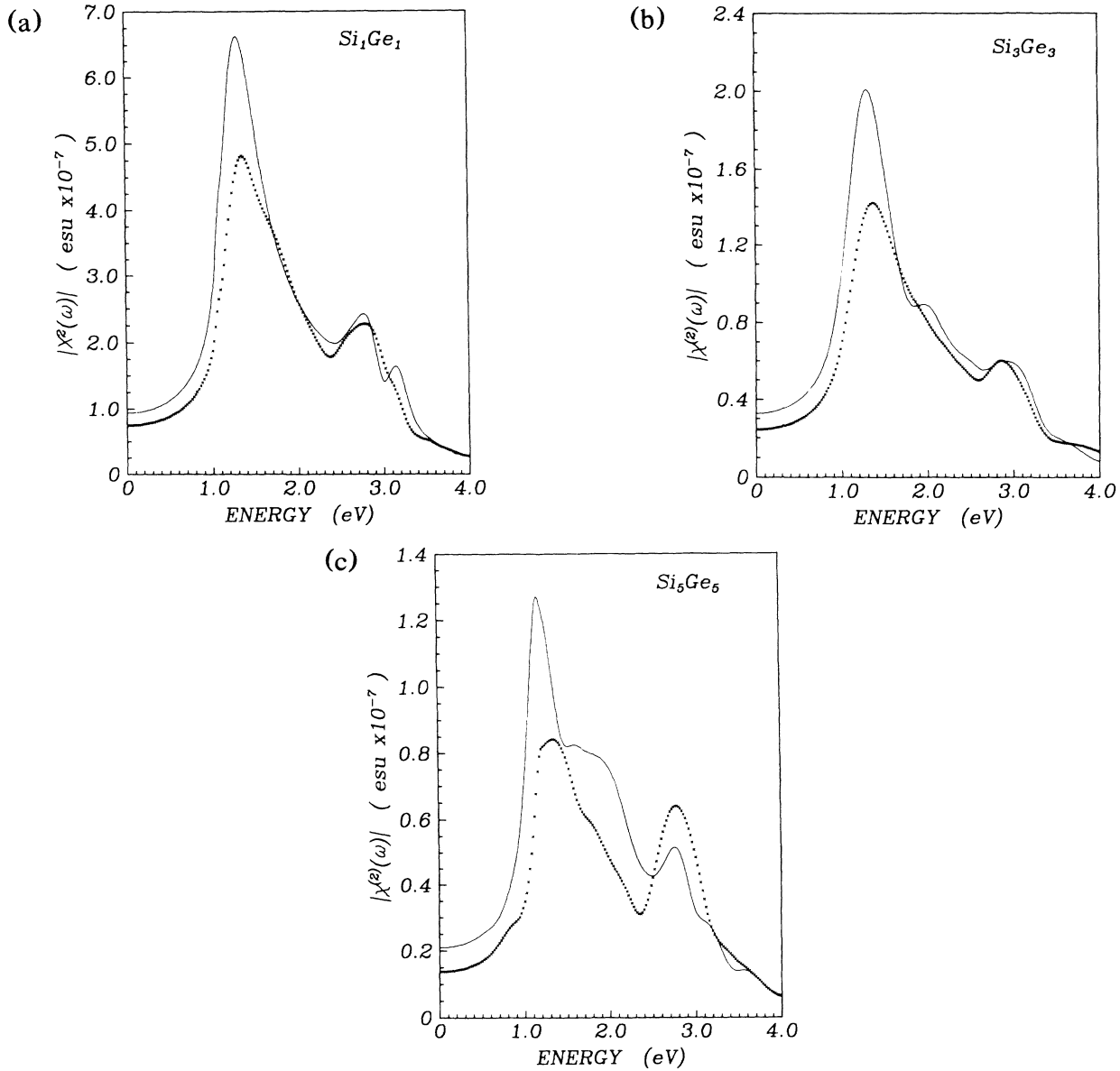


FIG. 1. Results for  $|\chi^{(2)}(-2\omega; \omega, \omega)|$  for (a)  $n=1$ , (b)  $n=3$ , and (c)  $n=5$  [solid lines,  $\chi_{123}^{(2)}(\omega)$ ; crosses,  $\chi_{321}^{(2)}(\omega)$ ].

in Fig. 2. The curves extracted from the different superlattice calculations are in good agreement. The discrepancies arise because in this model SHG is assumed to arise entirely from the interfaces; since the interfaces in different superlattices are not exactly the same, it is then not surprising that the results predicted for an isolated interface are slightly different. Nonetheless, this is the first indication of the magnitude and frequency dependence of SHG at a semiconductor interface.

Returning to our superlattice results (Fig. 1), we note that there is a reasonably large SHG response even below 1.16 eV, the minimal (indirect) bandgap of Si which is typically used as a substrate and spacing material for these superlattices.<sup>7,8</sup> It should be possible,

therefore, to measure  $\chi^{(2)}$  below this energy, since there would be no loss of the pump beam intensity due to linear absorption in the Si. Since the indirect absorption is weak at energies up to 1.7 eV (Ref. 11), one should be able to detect most of the structure even at these ener-

TABLE I. Theoretical results for  $\chi^{(2)}(0)$  in units of  $10^{-8}$  esu.

Component	Si <sub>1</sub> Ge <sub>1</sub>	Si <sub>3</sub> Ge <sub>3</sub>	Si <sub>5</sub> Ge <sub>5</sub>
$\chi_{123}^{(2)}(0)$	9.4	3.3	2.1
$\chi_{321}^{(2)}(0)$	7.5	2.4	1.4

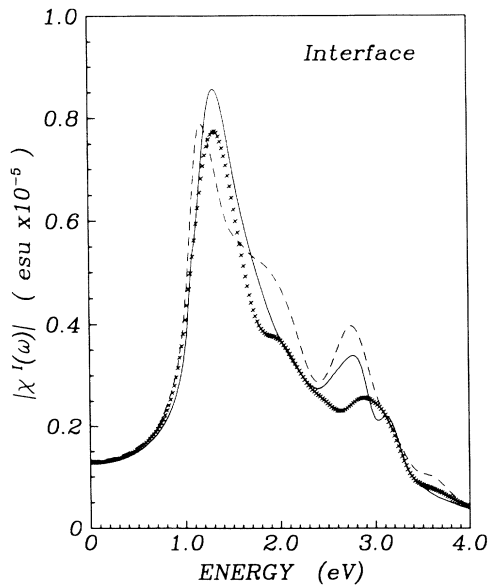


FIG. 2. Results for SHG at interfaces (solid line,  $n=1$ ; crosses,  $n=3$ ; and dashed line,  $n=5$ ).

gies. Finally, we note that even for  $\text{Si}_5\text{Ge}_5$  the predicted  $\chi^{(2)}$  is within an order of magnitude of that for GaAs, and so it should completely dominate the smaller quadrupole and magnetic-dipole-like terms which are present even in materials with inversion symmetry.

In conclusion, we have performed for the first time a full band-structure calculation of  $\chi^{(2)}(-2\omega; \omega, \omega)$  for the odd-period, strained,  $(\text{Si})_n/(\text{Ge})_n$  superlattices. The

response is comparable to the corresponding response of zinc-blende materials, and should be experimentally observable. We have also shown that the response can, in large part, be understood as arising from Si-Ge bonds where the inversion symmetry is broken, and we have used this to obtain an estimate for the SHG at an Si/Ge interface.

We gratefully acknowledge research support from the Natural Sciences and Engineering Research Council of Canada. This work was partially supported by the Ontario Laser and Lightwave Research Centre.

<sup>1</sup>Y. R. Shen, *J. Vac. Technol. B* **3**, 1464 (1985); *Annu. Rev. Mater. Sci.* **16**, 69 (1986); *Nature (London)* **337**, 519 (1989).

<sup>2</sup>G. L. Richmond, J. M. Robinson, and V. L. Shannon, *Prog. Surf. Sci.* **28**, 1 (1988).

<sup>3</sup>A. Liebsch, *Phys. Rev. Lett.* **61**, 1233 (1988).

<sup>4</sup>J. Rudnick and E. A. Stern, *Phys. Rev. B* **4**, 4274 (1971).

<sup>5</sup>Y. R. Shen, *Annu. Rev. Phys. Chem.* **40**, 327 (1989).

<sup>6</sup>E. Ghaharamani, D. J. Moss, and J. E. Sipe, *Phys. Rev. B* **41**, 5112 (1990).

<sup>7</sup>T. P. Pearsall, J. Bevk, L. C. Feldman, J. M. Bonar, J. P. Mannaerts, and A. Ourmazd, *Phys. Rev. Lett.* **58**, 729 (1987).

<sup>8</sup>M. S. Hybertsen, M. Schlüter, R. People, S. A. Jackson, D. V. Lang, T. P. Pearsall, J. C. Bean, J. M. Vandenberg, and J. Bevk, *Phys. Rev. B* **37**, 10195 (1988).

<sup>9</sup>D. J. Moss, E. Ghaharamani, J. E. Sipe, and H. M. van Driel, *Phys. Rev. B* **41**, 1542 (1990).

<sup>10</sup>D. E. Aspnes, *Phys. Rev. B* **6**, 4648 (1972).

<sup>11</sup>D. E. Aspnes and A. A. Studna, *Phys. Rev. B* **27**, 985 (1983).